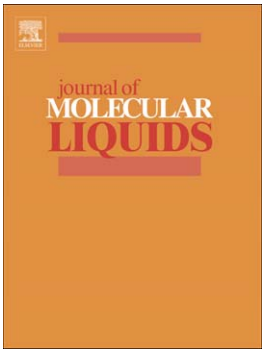

Influence of homogeneous-heterogeneous reactions on MHD 3D Maxwell fluid flow with Cattaneo-Christov heat flux and convective boundary condition

M. Ramzan, M. Bilal, Jae Dong Chung

PII: S0167-7322(16)33451-1
DOI: doi: 10.1016/j.molliq.2017.01.061
Reference: MOLLIQ 6863

To appear in: *Journal of Molecular Liquids*

Received date: 2 November 2016
Revised date: 1 January 2017
Accepted date: 17 January 2017

Please cite this article as: M. Ramzan, M. Bilal, Jae Dong Chung, Influence of homogeneous-heterogeneous reactions on MHD 3D Maxwell fluid flow with Cattaneo-Christov heat flux and convective boundary condition, *Journal of Molecular Liquids* (2017), doi: 10.1016/j.molliq.2017.01.061

Influence of homogeneous-heterogeneous reactions on MHD 3D Maxwell fluid flow with Cattaneo-Christov heat flux and convective boundary condition

M. Ramzan[a,1], M. Bilal[b], Jae Dong Chung[c],

[a] *Department of Computer Science, Bahria University, Islamabad Campus, Islamabad, 44000, Pakistan.*

[b] *Department of Mathematics, Faculty of Computing, Capital University of Science and Technology, Islamabad, Pakistan.*

[c] *Department of Mechanical Engineering, Sejong University, Seoul 143-747, Korea.*

Abstract: This study examines the effect of Cattaneo Christov heat flux with heat generation/absorption on three dimensional Maxwell fluid flow past a bidirectional stretched surface in the presence of magnetohydrodynamic (MHD. The effects of homogeneous−heterogeneous reactions with convective boundary condition are also taken into account. Analytical solution of nonlinear differential equations is obtained by employing Homotopy Analysis method. Graphical illustrations displaying effects of sundry parameters with required discussion highlighting their physical impact are also a part of this exploration. It is perceived that velocity distributions are decreasing functions of Hartmann number. Moreover, increasing values of measure of homogeneous reaction parameter reduces concentration distribution.

Keywords: Homogenous-Heterogeneous reactions; Magnetic field; Cattaneo-Christov heat flux model; Convective boundary condition; Heat generation/absorption.

1 Introduction

Heat transfer analysis is a subject of great interest for scientists and researches due to its viability in numerous industrial and engineering applications like electronic devices, nuclear reactors' cooling, power generation, and heat conduction in tissues etc. Pioneering work by

[1]Corresponding Author's email address: mramzan@bahria.edu.pk

Fourier [1] regarding heat transfer process is considered to be the most effective model due to its applicability in varied circumstances. Cattaneo [2] addressed the flaw in Fourier's model by inserting the time relaxation term to get rid of inconsistency in heat conduction, named as "Paradox of heat conduction". Christov [3] improved Cattaneo's model by considering Oldroyd's upper-convected derivative for ordinary derivative. The uniqueness of the solution using Cattaneo-Christov model for incompressible fluid was proved by Tibullo and Zampoli [4]. Han et al. [5] discussed upper-convected Maxwell fluid flow with slip condition in attendance of Cattaneo-Christov heat flux. Recently, researchers and scientists have shown great interest in exploring new avenues regarding Cattaneo-Christov heat flux model [6 − 10].

The study of flows with effects of magnetohydrodynamic (MHD) are imperative due to its wide range applications like gas turbine, solar power, plasma studies, nuclear power plants and in magnetic resonance imaging (MRI) etc. Precisely, MHD flows with convective boundary conditions have special importance in many engineering applications like thermal energy storage, processes involving high temperatures, and space vehicle re-entry etc. Ibrahim and Haq [11] studied the flow of nanofluid under the effects of convective boundary condition and magnetohydrodynamic past a stretching surface. Ramzan et al. [12] examined micropolar fluid flow with MHD, joule heating in addition to convective boundary condition and thermal radiation effects. A similar study was carried out by Waqas et al. [13] considering MHD mixed convective micropolar fluid flow with convective boundary condition past a nonlinear stretched surface. Hussain et al. [14] found analytical solution of MHD Casson nanofluid flow with convective boundary conditions and viscous dissipation. Mabood et al. [15] explored effects of MHD and convective boundary condition on stagnation point nanoparticle flow with suction/injection. Recent attempts highlighting magnetohydrodynamics effects with varied features may include [16 − 26].

In numerous engineering and technological applications, importance of non-Newtonian fluids cannot be negated. Examples of these materials may include shampoos, mayonnaise, blood, paints, alcoholic beverages, yogurt, cosmetics, and syrups etc. Mathematical modelling of these fluids is very tedious as typical Navier-Stokes equations are not enough to express characteristics of non-Newtonian fluids. These fluids are categories as differential, rate and

integral types. Maxwell fluid fall in the category of rate type fluids and is used to describe features of relaxation time.

The present exploration describes the impact homogeneous-heterogeneous reactions on three dimensional MHD Maxwell fluid flow with Cattaneo-Christov heat flux past a bidirectional stretched surface. Here, in this paper the novelty is twofold:

i) Combined effects of homogeneous-heterogeneous reactions on 3D flow of Maxwell fluid with Cattaneo-Christov heat flux are being presented first time.

ii) Variable temperature dependent thermal conductivity for three dimensional Cattaneo-Christov heat flux model with MHD and convective boundary condition are also considered.

Series solutions for involved distributions are acquired using Homotopy Analysis method (HAM) [27 – 29]. Graphical illustrations highlighting varied prominent parameters' effects with their physical importance are also given.

2 Mathematical formulation

Consider 3D flow of MHD Maxwell fluid with Cattaneo-Christov heat flux and homogeneous-heterogeneous reactions past a bidirectional stretched surface. The fluid occupies the region $z \geq 0$ whereas $u = ax$ and $v = by$ are stretching velocities in x and y directions respectively as shown in fig. 1. Temperature at the surface T_w is greater than the temperature far-off from the surface T_∞. Presence of uniform magnetic field makes the fluid electrically conducting. However, induced magnetic field is ignored due to our supposition of small Reynolds number. The homogeneous and heterogeneous reactions taken on boundary layer flow and on the catalyst surface respectively are represented by

$$A + 2B \rightarrow 3B, \text{ rate } = k_c a b^2, \tag{1}$$

and

$$A \rightarrow B, \text{ rate } = k_s a. \tag{2}$$

Here, chemical species A and B have concentrations a and b with rate constants k_c and k_s respectively. It is assumed that there is no variation in the temperature for the both under consideration reactions. Governing equations of the existing flow under all assumptions discussed above are given by [30, 31]

$$\frac{\partial u}{\partial x}+\frac{\partial v}{\partial y}+\frac{\partial w}{\partial z}=0, \tag{3}$$

$$u\frac{\partial u}{\partial x}+v\frac{\partial u}{\partial y}+w\frac{\partial u}{\partial z}+\lambda_1\left(\begin{array}{c} u^2\frac{\partial^2 u}{\partial x^2}+v^2\frac{\partial^2 u}{\partial y^2}+w^2\frac{\partial^2 u}{\partial z^2}+ \\ 2uv\frac{\partial^2 u}{\partial x\partial y}+2vw\frac{\partial^2 u}{\partial y\partial z}+2uw\frac{\partial^2 u}{\partial x\partial z}\end{array}\right)=\nu\frac{\partial^2 u}{\partial z^2}-\frac{\sigma B_o^2}{\rho}\left(u+\lambda_1 w\frac{\partial u}{\partial z}\right), \tag{4}$$

$$u\frac{\partial v}{\partial x}+v\frac{\partial v}{\partial y}+w\frac{\partial v}{\partial z}+\lambda_1\left(\begin{array}{c} u^2\frac{\partial^2 v}{\partial x^2}+v^2\frac{\partial^2 v}{\partial y^2}+w^2\frac{\partial^2 v}{\partial z^2}+ \\ 2uv\frac{\partial^2 v}{\partial x\partial y}+2vw\frac{\partial^2 v}{\partial y\partial z}+2uw\frac{\partial^2 v}{\partial x\partial z}\end{array}\right)=\nu\frac{\partial^2 v}{\partial z^2}-\frac{\sigma B_o^2}{\rho}\left(v+\lambda_1 w\frac{\partial v}{\partial z}\right), \tag{5}$$

$$\rho C_P\mathbf{V}.\nabla T=-\nabla.\mathbf{q}, \tag{6}$$

$$u\frac{\partial a}{\partial x}+v\frac{\partial a}{\partial y}+w\frac{\partial a}{\partial z}=D_A\frac{\partial^2 a}{\partial z^2}-k_c ab^2,$$

$$u\frac{\partial b}{\partial x}+v\frac{\partial b}{\partial y}+w\frac{\partial b}{\partial w}=D_B\frac{\partial^2 b}{\partial z^2}+k_c ab^2, \tag{7}$$

where ν, σ, B_0, T, C_p, ρ, v, λ_1 , D_A and D_B, k_c and k_s, $\mathbf{q}$ and (u, v) are kinematic viscosity, electrical conductivity, uniform magnetic field, temperature, specific heat, fluid density, kinematic viscosity, relaxation time, diffusion coefficients, rate constants, heat flux and velocities along (x, y) directions respectively. The heat flux $\mathbf{q}$ satisfy the following relation

$$\mathbf{q}+\lambda_2\left(\frac{\partial \mathbf{q}}{\partial t}+\mathbf{V}.\nabla\mathbf{q}-\mathbf{q}.\nabla\mathbf{V}+(\nabla.\mathbf{V})\,\mathbf{q}\right)=-k\nabla T, \tag{8}$$

with k and λ_2 are fluid thermal conductivity and thermal relaxation time. Eliminating $\mathbf{q}$ from Eqs. (6) and (8) by taking into account [3],we get

$$u\frac{\partial T}{\partial x}+v\frac{\partial T}{\partial y}++w\frac{\partial T}{\partial z}=\frac{1}{\rho C_P}\frac{\partial}{\partial z}\left(k\frac{\partial T}{\partial z}\right)$$

$$-\lambda_2\left(\begin{array}{c} u^2\frac{\partial^2 T}{\partial x^2}+v^2\frac{\partial^2 T}{\partial y^2}+w^2\frac{\partial^2 T}{\partial z^2}+2uv\frac{\partial^2 T}{\partial x\partial y} \\ +2vw\frac{\partial^2 T}{\partial y\partial z}+2uw\frac{\partial^2 T}{\partial x\partial z}+\left(u\frac{\partial u}{\partial x}+v\frac{\partial u}{\partial y}+w\frac{\partial u}{\partial z}\right)\frac{\partial T}{\partial x}+ \\ \left(u\frac{\partial v}{\partial x}+v\frac{\partial v}{\partial y}+w\frac{\partial v}{\partial z}\right)\frac{\partial T}{\partial y}+\left(u\frac{\partial w}{\partial x}+v\frac{\partial w}{\partial y}+w\frac{\partial w}{\partial z}\right)\frac{\partial T}{\partial z} \end{array}\right)+\frac{Q}{\rho C_P}\left(T-T_\infty\right). \quad (9)$$

The problem supporting boundary conditions are given by

$$\begin{aligned} u &= cx,\ v=by, w=0\ -k_h\frac{\partial T}{\partial z}=h_f\left(T_w-T\right), \\ D_A\frac{\partial a}{\partial z} &= k_s a,\ D_B\frac{\partial b}{\partial z}=-k_s a,\ \text{at}\ \ z=0, \end{aligned}$$

$$u\to 0,\ v\to 0,\ a\to a_o,\ b\to 0,\ \ T\to T_\infty \quad \text{as}\ z\to\infty. \quad (10)$$

where $h_f,\ k_h$ and c, b, a, a_0 are heat transfer coefficient, thermal conductivity of the fluid and positive dimensional constants.

Assuming the following transformations and using the variable thermal conductivity [30] in Eq. (9)

$$\begin{aligned} u &= cxf'(\eta),\ v=cyg'(\eta),\ w=-\sqrt{c\nu}\left(f(\eta)+g(\eta)\right), k=k_\infty\left(1+\epsilon\theta\right) \\ \theta(\eta) &= \frac{T-T_\infty}{T_w-T_\infty},\ \eta=\sqrt{\frac{c}{\nu}}y,\ b=a_0 h(\eta), a=a_0\phi(\eta). \end{aligned} \quad (11)$$

Eq. (3) is automatically satisfied, however Eqs. (4), (5), (7), (9) and (10) take the form

$$f'''+K_1\left(2\left(f+g\right)f'f''-\left(f+g\right)^2 f'''\right)+\left(f+g\right)f''-f'^2-M^2\left(f'-K_1\left(f+g\right)f''\right)=0, \quad (12)$$

$$g'''+K_1\left(2\left(f+g\right)g'g''-\left(f+g\right)^2 g'''\right)+\left(f+g\right)g''-g'^2-M^2\left(g'-K_1\left(f+g\right)g''\right)=0, \quad (13)$$

$$\left(1+\epsilon\theta\right)\theta''+\epsilon\theta'^2+\Pr\left(f+g\right)\theta'-\Pr K_2\left(\left(f+g\right)^2\theta''+\left(f+g\right)\left(f'+g'\right)\theta'\right)+\Pr S\theta=0, \quad (14)$$

$$\phi''+Sc\left(f+g\right)\phi'-ScK_3\phi h^2=0, \quad (15)$$

$$\delta h''+Sc\left(f+g\right)h'+ScK_3\phi h^2=0, \quad (16)$$

$$\begin{aligned} f(0) &= 0, \quad f'(0)=1,\ g(0)=0, \quad g'(0)=\lambda,\ \phi'(0)=\gamma_2\,\phi(0), \\ \theta'(0) &= -\gamma_1\,(1-\theta(0)), \quad \delta h'(0)=\gamma_2\,\phi(0) \quad \text{at} \quad y=0, \\ f'(\infty) &\to 0,\ g(\infty)\to 1, h(\infty)\to 1,\ \phi(\infty)\to 1,\ \theta(\infty)\to 0, \text{ as } y\to\infty, \end{aligned} \tag{17}$$

where Pr, K_1, ϵ, M, λ, Sc, γ_2, K_3, K_2, S, δ and γ_1 are the Prandtl number, Deborah number with respect to relaxation time, thermal conductivity parameter, Hartmann number, ratio of stretching rates, Schmidt number, measure of the strength of the heterogeneous reaction, measure of strength of homogenous reaction, Deborah number with respect to relaxation time of heat flux, heat generation parameter, ratio of diffusion coefficient and Biot number respectively . The values of these parameters are given below:

$$\begin{aligned} \Pr &= \frac{\mu C_p}{k}, \quad K_1=\lambda_1 c\ , \quad K_2=\lambda_2 c, \quad S=\frac{Q}{\rho c C_p}, \quad K_3=\frac{k_c a_0^2}{a}, \quad \delta=\frac{D_B}{D_A}, \\ \gamma_1 &= \frac{h_f}{k}\sqrt{\frac{\nu}{c}}, \ M=\frac{\sigma B_o^2}{c\rho}, \quad Sc=\frac{\nu}{D_A}, \quad \gamma_2=\frac{k}{D_A a_0}\sqrt{\frac{c}{\nu}}, \quad \lambda=\frac{b}{c}, \epsilon=\frac{k_w-k_\infty}{k_\infty}. \end{aligned} \tag{18}$$

Considering that the diffusion coefficients of chemical species A and B are comparable in size, it leads us to assume D_A and D_B are also same. i.e. $\delta=1$. So, we have

$$\phi(\eta)\ + h(\eta) = 1. \tag{19}$$

Thus, Eqs. (15) and (16) take the form

$$\phi'' + Sc\,(f+g)\,\phi' - Sc\gamma_1\phi\,(1-\phi)^2 = 0, \tag{20}$$

with allied boundary conditions

$$\phi'(0)=\gamma_2\phi(0),\ \phi(\infty)=1. \tag{21}$$

Skin friction coefficients and local Nusselt number are represented by

$$C_{fx}=\frac{\tau_{wx}}{\rho u_w^2(x)},\ C_{fy}=\frac{\tau_{wy}}{\rho u_w^2(y)}\ ,\ Nu_x=\frac{x q_w}{k(T_w-T_\infty)}, \tag{22}$$

where τ_{wx}, τ_{wy} and q_w are given by:

$$\begin{aligned} \tau_{wx} &= \mu\left(1+K_1\right)\left(\frac{\partial u}{\partial z}\right)_{z=0}, \quad \tau_{wy}=\mu\left(1+K_1\right)\left(\frac{\partial v}{\partial z}\right)_{z=0}, \\ q_w &= -k\left(\frac{\partial T}{\partial z}\right)_{z=0}. \end{aligned} \tag{23}$$

Dimensionless forms of Eq.(23) are as under

$$C_{fx}Re_x^{1/2}=\left(1+K_1\right)f''\left(0\right),\ C_{fy}Re_x^{1/2}=\left(1+K_1\right)g''\left(0\right),\ Nu_{_x}Re_x^{-1/2}=-\theta'\left(0\right). \tag{24}$$

3 Homotopic solutions

The selection of initial guess estimates $(f_0, g_0, \theta_0, \phi_0)$ with respective operators $(\mathcal{L}_f, \mathcal{L}_g, \mathcal{L}_\theta, \mathcal{L}_\phi)$ is main to Homotopy Analysis method

$$\begin{aligned} f_0\left(\eta\right) &= \left(1-\exp\left(-\eta\right)\right),\ g_0\left(\eta\right)=\lambda(1-\exp\left(-\eta\right)), \\ \theta_0\left(\eta\right) &= \frac{\gamma_1\exp\left(-\eta\right)}{1+\gamma_1},\ \phi_0\left(\eta\right)=1-\frac{1}{2}\exp\left(-\gamma_2\eta\right)\ , \end{aligned} \tag{25}$$

and

$$\mathcal{L}_f\left(\eta\right)=\frac{d^3f}{d\eta^3}-\frac{df}{d\eta},\ \mathcal{L}_g\left(\eta\right)=\frac{d^3g}{d\eta^3}-\frac{dg}{d\eta},\ \mathcal{L}_\theta\left(\eta\right)=\frac{d^2\theta}{d\eta^2}-\theta,\ \mathcal{L}_\phi\left(\eta\right)=\frac{d^2\phi}{d\eta^2}-\phi. \tag{26}$$

Properties of these operators are appended below

$$\mathcal{L}_f\left[C_1+C_2\exp(\eta)+C_3\exp(-\eta)\right]=0,$$

$$\mathcal{L}_g\left[C_4+C_5\exp(\eta)+C_6\exp(-\eta)\right]=0,$$

$$\mathcal{L}_\theta\left[C_7\exp(\eta)+C_8\exp(-\eta)\right]=0,$$

$$\mathcal{L}_\phi\left[C_9\exp(\eta)+C_{10}\exp(-\eta)\right]=0, \tag{27}$$

where C_i $(i=1-10)$ are the arbitrary constants. These constants through boundary con-

ditions have the following values

$$\begin{aligned}
C_2 &= C_5 = C_7 = C_9 = 0, \qquad C_3 = \left.\frac{\partial f_m^\star(\eta)}{\partial \eta}\right|_{\eta=0}, \\
C_1 &= -C_3 - f_m^\star(0), \quad C_6 = \left.\frac{\partial g_m^\star(\eta)}{\partial \eta}\right|_{\eta=0}, \\
C_4 &= -C_6 - g_m^\star(0), \quad C_8 = \frac{1}{1+\gamma_1}\left(\left.\frac{\partial \theta_m^*(\eta)}{\partial \eta}\right|_{\eta=0} - \gamma_1 \theta_m^*(0)\right), \\
C_{10} &= \frac{1}{1+\gamma_2}\left(\left.\frac{\partial \phi_m^*(\eta)}{\partial \eta}\right|_{\eta=0} - \gamma_2 \phi_m^*(0)\right).
\end{aligned} \tag{28}$$

3.1 Convergence analysis

The auxiliary parameters play a vital role to establish the region of convergence for the series solutions. To define the same region, $\hbar$-curves are illustrated in Fig. 2. Acceptable ranges of these parameters $\hbar_f$, $\hbar_g$, $\hbar_\theta$ and $\hbar_\phi$ as displayed in figure are $-2.0 \leq \hbar_f \leq -0.5$, $-2.0 \leq \hbar_g \leq -0.4$, $-2.1 \leq \hbar_\theta \leq -0.5$ and $-2.0 \leq \hbar_\phi \leq -0.3$. Table 1. depicts the convergence ranges of these parameters to 35^{th} order of approximations, and all ranges are found in an excellent agreement to those portrayed in Fig. 2.

Table 1. Convergence of series solutions for varied order of approximations when $M = 0.4$, $\Pr = 2.0$, $\gamma_1 = 0.2$, $\gamma_2 = 0.4$, $Sc = 0.7$, $Sc = 0.2$, $K_1 = 0.2$, $K_2 = 0.3$, $K_3 = 0.3$, $\lambda = 0.3$, $\epsilon = 0.2$.

Order of approximations	$-f''(0)$	$-g''(0)$	$-\theta'(0)$	$\phi'(0)$
1	1.11907	0.27776	0.16619	0.19383
5	1.18870	0.28067	0.17327	0.18957
10	1.19875	0.28405	0.17576	0.18972
15	1.20153	0.28541	0.17530	0.19041
20	1.20275	0.28608	0.17469	0.19110
25	1.20341	0.28647	0.17442	0.19173
30	1.20365	0.28660	0.17430	0.19180
35	1.20368	0.28666	0.17428	0.19181
40	1.20368	0.28666	0.17428	0.19181

4 Results and Discussion

This section demonstrates the flow behavior of various arising parameters on velocity, temperature and concentration profiles. The case of viscous fluid may be extracted from Maxwell fluid model by considering Deborah number K_1 equal to zero. Effects of K_1 on the velocity and temperature profiles are shown in Figs. $(3-5)$. As Deborah number has a direct proportion to relaxation time, so higher values of relaxation time boosts Deborah number which resist fluid flow. That is why a reduction in velocity profiles is observed for higher values of Deborah number (Figs. 3 & 4). From Fig. 5, it is observed that temperature profile is snowballing function of Deborah number. It is an accepted truth that an increase in temperature profile and its associated boundary layer thickness is seen for higher Deborah number. Figs. 6 and 7 are drawn to portray the effects of Hartmann number M on both velocity distributions along x and $y-$directions. Decrease in both velocities is observed due to the resistance offered by Lorentz force. However, this resistive Lorentz force causes an enhancement in the temperature distribution (see Fig. 8). From Fig. 9, it is witnessed that higher values of heat generation/absorption parameter S cause an increase in temperature distribution. Actually, more heat is immersed by the fluid when we increase S. The impact of relaxation time of heat flux K_2 on temperature distribution is analyzed in Fig. 10. For

increasing values of relaxation time for heat flux, decreasing temperature profile is witnessed. From Fig. it is observed that temperature distribution turned out to be sharper in neighborhood of the boundary as K_2 mounted which is a sign of the development in wall slope of temperature field. Fig. 11 shows that concentration distribution and its associated solutal boundary layer thickness decrease for increasing values of "measure of homogeneous reaction parameter K_3". Since the reactants are utilized during homogeneous reaction that is why reduction in concentration profile is observed. Effect of "strength of heterogeneous reaction parameter γ_2 on concentration distribution is shown in Fig. 12. It is witnessed that for higher values of γ_2, diffusion decreases, and for the particles with low diffusion characteristics, concentration will be increased. Fig. 13 portrays the influence of ratio of stretching constant λ on concentration distribution. Here, concentration profile is an increasing function of λ. An increase in λ results in stretching of the sheet along $y-$axis, which ultimately boost the concentration of the fluid. In Fig. 14, impact of Prandtl number Pr on temperature field is displayed. Increasing values of Pr decrease fluid's thermal diffusivity which eventually lowers the temperature of the fluid. Fig. 15 demonstrates the influence of Biot number γ_1 on temperature profile, which shows that temperature is growing function of γ_1. Increasing values of γ_1 are due to larger heat transfer resistance inside a body as compared to surface. Which results in high temperature of the fluid. Fig. 16 represents the impact of Schmidt number Sc on concentration distribution. It can be seen that concentration distribution is mounting function of Sc. As Schmidt number is referred as the quotient of momentum diffusivity to mass diffusivity. Therefore, high momentum diffusivity as compared to mass diffusivity boosts the Sc. Which ultimately increase the concentration of the fluid. The variation of thermal conductivity parameter ϵ on temperature distribution is illustrated in Fig. 17. It is known fact that higher thermal conductivity boosts the thermal boundary layer. The effect is reflected in Fig.17. Effects of Deborah number with respect to relaxation time K_1 and Hartmann number M on Skin friction coefficient are portrayed in Fig. 18. It is perceived that Skin friction coefficient is an increasing function of both K_1 and M. Similarly, local Nusselt number also increases for higher values of Prandtl number Pr and Deborah number K_1 with respect to relaxation time of heat flux K_2 (Fig. 19).

Table 2 depicts local Nusselt number in the absence of MHD, Cattaneo Christov heat flux, heat generation/absorption and homogeneous heterogeneous reactions for different values of various parameters. It is observed that all obtained values of local Nusselt number are in an excellent agreement with the values found in Hayat et al. [32].

Table 2. Values of local Nusselt number $-\theta'(0)$ in the absence of MHD, Cattaneo Christov heat flux, heat generation/absorption and homogeneous heterogeneous for the varied values of the parameters reactions K_1, and Pr when $\gamma_1 = 0.6$.

K_1	λ	Pr	[32]	Present
0.0	0.5	1.0	0.33040	0.33040
0.3			0.32160	0.32160
0.8			0.30799	0.30799
1.2			0.29873	0.29873
0.4	0.0		0.28908	0.28908
	0.4		0.31664	0.31664
	0.7		0.33017	0.33017
	1.0		0.34070	0.34070
		0.7	0.28279	0.28279
		1.2	0.34042	0.34042
		1.6	0.36840	0.36840
		2.0	0.38887	0.38887

5 Concluding Remarks

Present exploration examines the homogeneous heterogeneous reactions on three dimensional Maxwell fluid flow past a bidirectional stretched surface, with magnetohydrodynamic and heat generation/absorption. Effects of Cattaneo Christov heat flux with convective boundary condition are also considered. Homotopy Analysis method is engaged to find solve the modeled problem. Significant findings of the problem are:

- Reduction in velocity distributions is witnessed for higher values of Deborah number.

- Velocity distributions are decreasing functions of Hartmann number.
- Increasing values of measure of homogeneous reaction parameter reduces concentration distribution.
- Temperature field is growing function Biot number.
- Heat generation/absorption parameter causes an increase in temperature distribution.

Conflict of Interest: Authors have no conflict of interest regarding this publication.

Acknowledgments: This research is supported by Korea Institute of Energy Technology Evaluation and Planning (KETEP) granted financial resource from the Ministry of Trade, Industry & Energy of Korea (No. 20132010101780).

References

[1] J. B. J. Fourier, *Théorie analytique ee la chaleur*, Paris, 1822.

[2] C. Cattaneo, Sulla conduzione del calore, Atti. Semin. Mat. Fis Univ. Modena Reggio Emilia 3 (1948) 83–101.

[3] C. I. Christov, On frame indifferent formulation of the Maxwell–Cattaneo model of finite-speed heat conduction, Mechanics Research Communications, 36 (2009) 481–486.

[4] V. Tibullo, V. Zampoli, A uniqueness result for the Cattaneo–Christov heat conduction model applied to incompressible fluids, Mechanics Research Communications, 38(1) (2011) 77–79.

[5] S. Han, L. Zheng, C. Li, X. Zhang, Coupled flow and heat transfer in viscoelastic fluid with Cattaneo–Christov heat flux model, Applied Mathematics Letters, 38 (2014) 87–93.

[6] J. A. Khan, M. Mustafa, T. Hayat, A. Alsaedi, Numerical study of Cattaneo-Christov heat flux model for viscoelastic flow due to an exponentially stretching surface, PLoS ONE, 10(9) (2015) e0137363.

[7] T. Hayat, T. Muhammad, A. Alsaedi, M. Mustafa, A comparative study for flow of viscoelastic fluids with Cattaneo-Christov heat flux, PLoS ONE, 11(5) (2016) e0155185.

[8] M. Ramzan, M. Bilal, J. D. Chung, Effects of MHD homogeneous-heterogeneous reactions on third grade fluid flow with Cattaneo-Christov heat flux, Journal of Molecular Liquids, 223 (2016) 1284–1290.

[9] T. Hayat, M. Imtiaz, A. Alsaedi, S. Almezal, On Cattaneo–Christov heat flux in MHD flow of Oldroyd-B fluid with homogeneous–heterogeneous reactions, Journal of Magnetism and Magnetic Materials, 401 (2016) 296–303.

[10] S. A. Shehzad, F. M. Abbasi, T. Hayat, A. Alsaedi, Cattaneo-Christov heat flux model for Darcy-Forchheimer flow of an Oldroyd-B fluid with variable conductivity and nonlinear convection, Journal of Molecular Liquids, 224 (2016) 274–278.

[11] W. Ibrahim, R. U. Haq, Magnetohydrodynamic (MHD) stagnation point flow of nanofluid past a stretching sheet with convective boundary condition, Journal of the Brazilian Society of Mechanical Sciences and Engineering, 38(4) (2016) 1155–1164.

[12] M. Ramzan, M. Farooq, T. Hayat, J. D. Chung, Radiative and Joule heating effects in the MHD flow of a micropolar fluid with partial slip and convective boundary condition, Journal of Molecular Liquids, 221 (2016) 394–400.

[13] M. Waqas, M. Farooq, M. I. Khan, A. Alsaedi, T. Hayat, T. Yasmeen, Magnetohydrodynamic (MHD) mixed convection flow of micropolar liquid due to nonlinear stretched sheet with convective condition, International Journal of Heat and Mass Transfer, 102 (2016) 766–772.

[14] T. Hussain, S. A. Shehzad, A. Alsaedi, T. Hayat, M. Ramzan, Flow of Casson nanofluid with viscous dissipation and convective conditions: A mathematical model, Journal of Central South University, 22 (2015) 1132−1140.

[15] F. Mabood, N. Pochai, S. Shateyi, Stagnation point flow of nanofluid over a moving plate with convective boundary condition and magnetohydrodynamics, Journal of Engineering, 2016 (2016) 5874864.

[16] A. Zeeshan, A. Majeed, R. Ellahi, Effect of magnetic dipole on viscous ferro-fluid past a stretching surface with thermal radiation, Journal of Molecular Liquids, 215 (2016) 549-554.

[17] M. M. Bhatti, R. Ellahi, A. Zeeshan, Study of variable magnetic field on the peristaltic flow of Jeffrey fluid in a non-uniform rectangular duct having compliant walls, Journal of Molecular Liquids, 222 (2016) 101-108.

[18] A. Majeed, A. Zeeshan, R. Ellahi, Unsteady ferromagnetic liquid flow and heat transfer analysis over a stretching sheet with the effect of dipole and prescribed heat flux, Journal of Molecular Liquids, 223 (2016) 528–533.

[19] R. Ellahi, The effects of MHD and temperature dependent viscosity on the flow of non-Newtonian nanofluid in a pipe: Analytical solutions, Applied Mathematical Modelling, 37 (3) (2013) 1451-1467.

[20] R Ellahi, E Shivanian, S Abbasbandy, T. Hayat, Numerical study of magnetohydrodynamics generalized Couette flow of Eyring-Powell fluid with heat transfer and slip condition, International Journal of Numerical Methods for Heat & Fluid Flow, 26 (5) (2016) 1433-1445.

[21] R. Ul Haq, S. Nadeem, Z. H. Khan, N. S. Akbar, Thermal radiation and slip effects on MHD stagnation point flow of nanofluid over a stretching sheet, Physica-E 65 (2015) 17-23.

[22] A. U. Khan, S. Nadeem, S. T. Hussain, Phase flow study of MHD nanofluid with slip effects on oscillatory oblique stagnation point flow in view of inclined magnetic field, Journal of Molecular Liquids 224 (2016) 1210-1219.

[23] R. Ul Haq, S. Nadeem, Z. H. Khan, N. F. M. Noor, Convective heat transfer in MHD slip flow over a stretching surface in the presence of carbon nanotubes, Physica-B 457 (2015) 40-47.

[24] S. Nadeem, R. Mehmood, N. S. Akbar, Combined effects of magnetic field and partial slip on obliquely striking rheological fluid over a stretching surface, Journal of Magnetism and Magnetic Materials 378 (2015) 457-462.

[25] A. A. Khan, S. Muhammad, R. Ellahi, Q. M. Z. Zia, Bionic Study of Variable Viscosity on MHD Peristaltic Flow of Pseudoplastic Fluid in an Asymmetric Channel, Journal of Magnetics 21(2) (2016) 273-280.

[26] R. Ellahi, S. U. Rahman, S. Nadeem, K. Vafai, The Blood Flow of Prandtl Fluid Through a Tapered Stenosed Arteries in Permeable Walls with Magnetic Field, Communications in Theoretical Physics, 63(3) (2015) 353-358.

[27] M. Ramzan, Influence of Newtonian heating on three dimensional MHD flow of couple stress nanofluid with viscous dissipation and joule heating, PLoS ONE 10 (4) (2015) e0124699.

[28] M Ramzan, M Bilal, Three-dimensional flow of an elastico-viscous nanofluid with chemical reaction and magnetic field effects, Journal of Molecular Liquids, 215 (2016) 212−220.

[29] M. Ramzan, M. Bilal, Time dependent MHD nano-second grade fluid flow induced by permeable vertical sheet with mixed convection and thermal radiation, PLoS ONE 10 (5) (2015) e0124929.

[30] F. M. Abbasi, S. A. Shehzad, Heat transfer analysis for three-dimensional flow of Maxwell fluid with temperature dependent thermal conductivity: Application of Cattaneo-Christov heat flux model, Journal of Molecular Liquids, 220 (2016) 848-854.

[31] T. Hayat, M. Imtiaz, S. Almezal, Modeling and analysis for three-dimensional flow with homogeneous-heterogeneous reactions, AIP Advances 5, (2015) 107209.

[32] T. Hayat, S. A. Shehzad, A. Alsaedi, Study on three-dimensional flow of Maxwell fluid over a stretching surface with convective boundary conditions, International Journal of the Physical Sciences, 7(5) (2012) 761− 768.

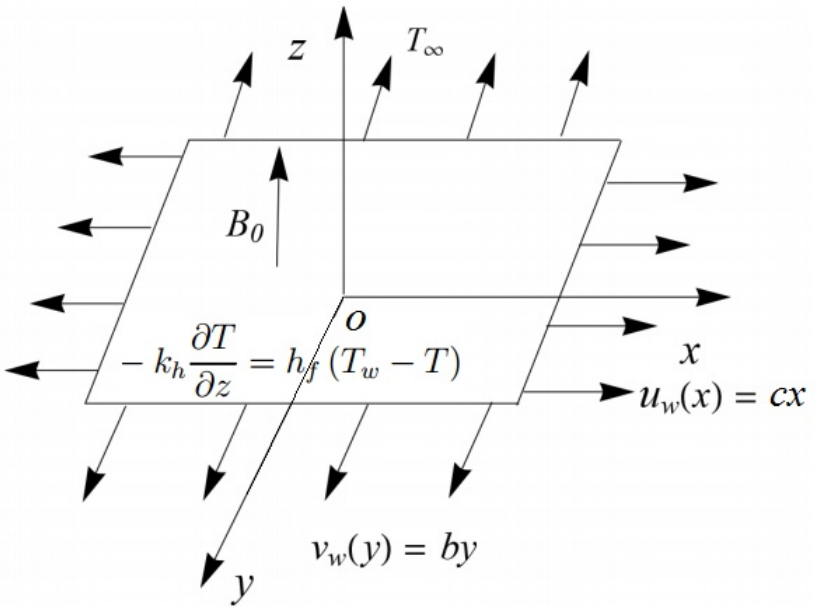

Fig. 1: Flow diagram

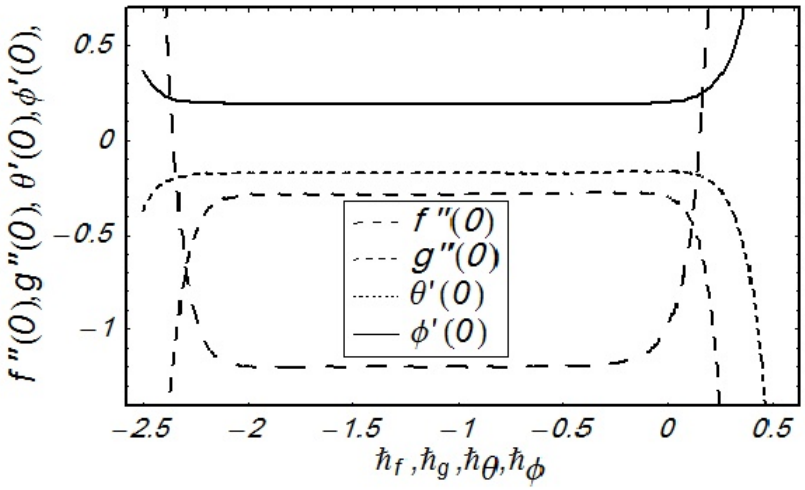

Fig. 2: $\hbar$-curves for function f, g, θ and ϕ

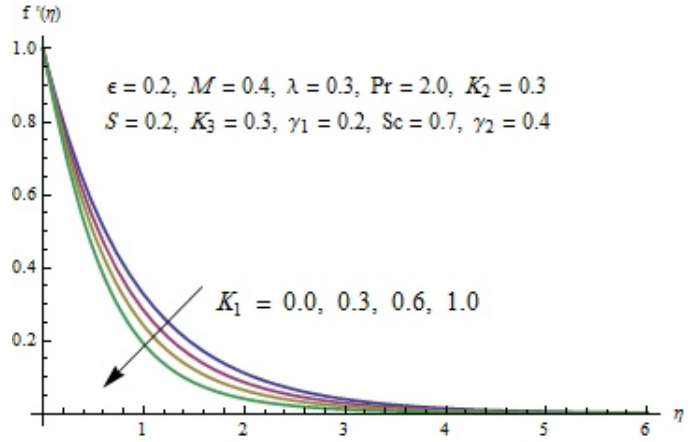

Fig. 3: Effect of K_1 on $f'(\eta)$

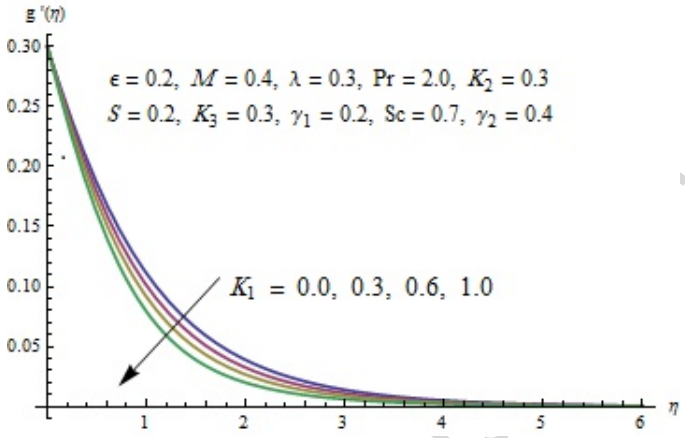

Fig. 4: Effect of K_1 on $g'(\eta)$

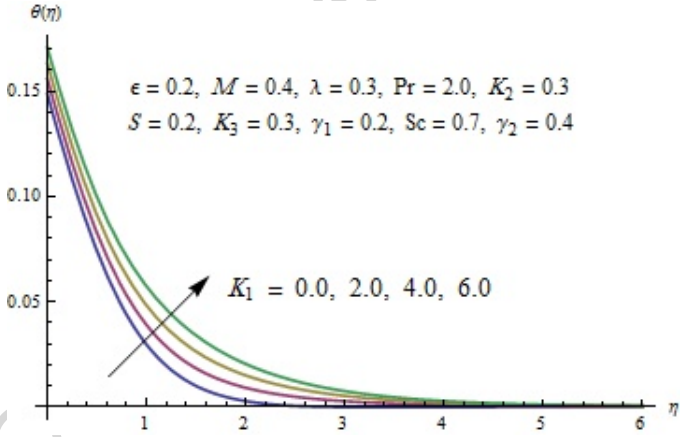

Fig. 5: Effect of K_1 on $\theta(\eta)$

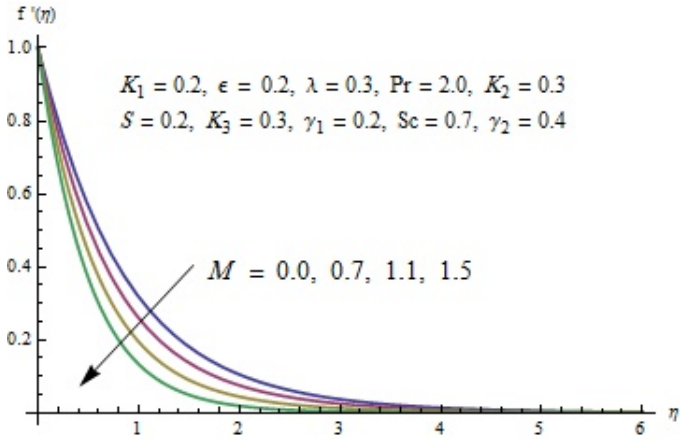

Fig. 6: Effect of M on $f'(\eta)$

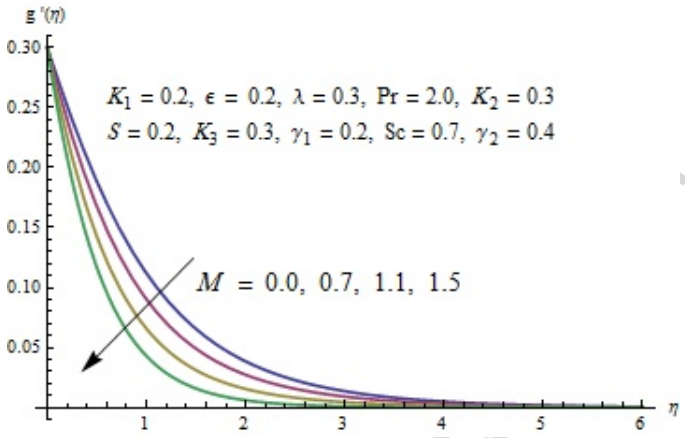

Fig. 7: Effect of M on $g'(\eta)$

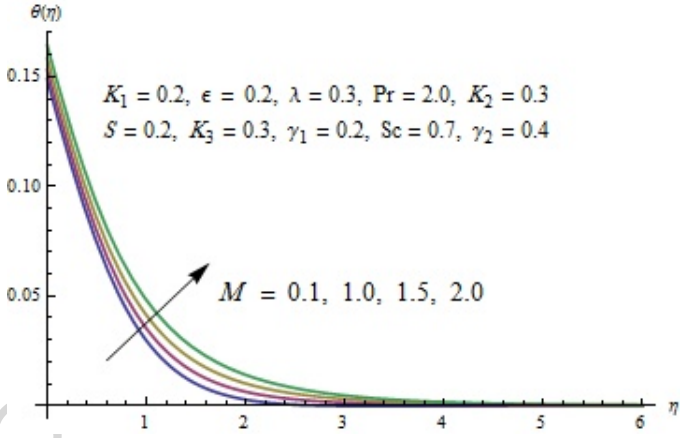

Fig. 8: Effect of M on $\theta(\eta)$

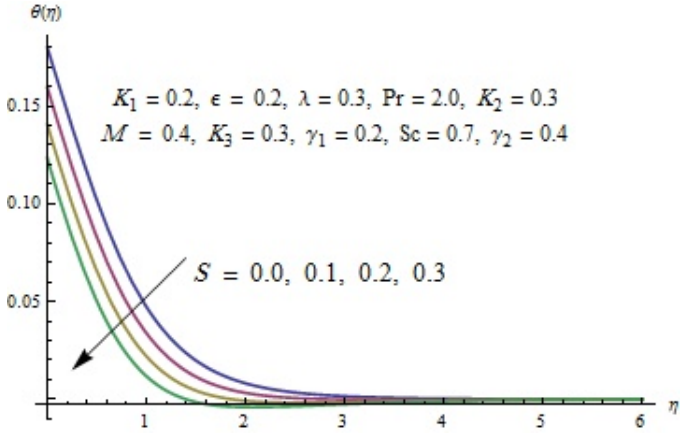

Fig. 9: Effect of S on $\theta(\eta)$

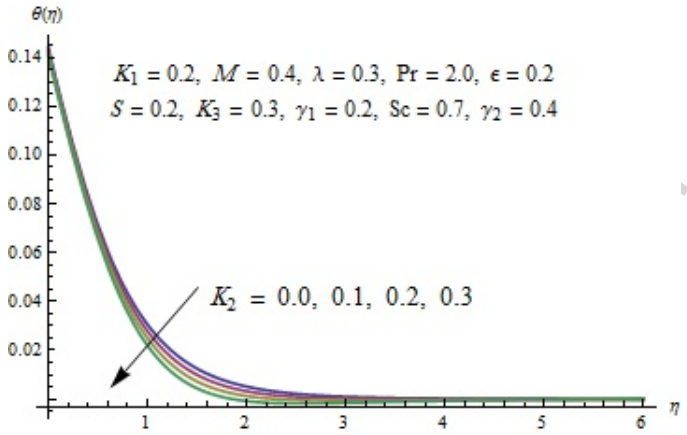

Fig. 10: Effect of K_2 on $\theta(\eta)$

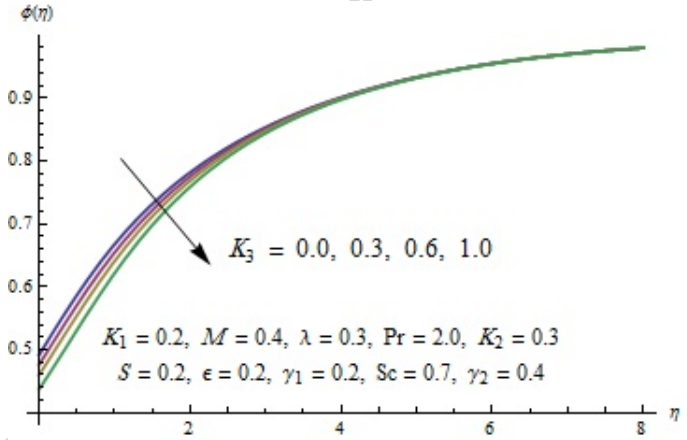

Fig. 11: Effect of K_3 on $\phi(\eta)$

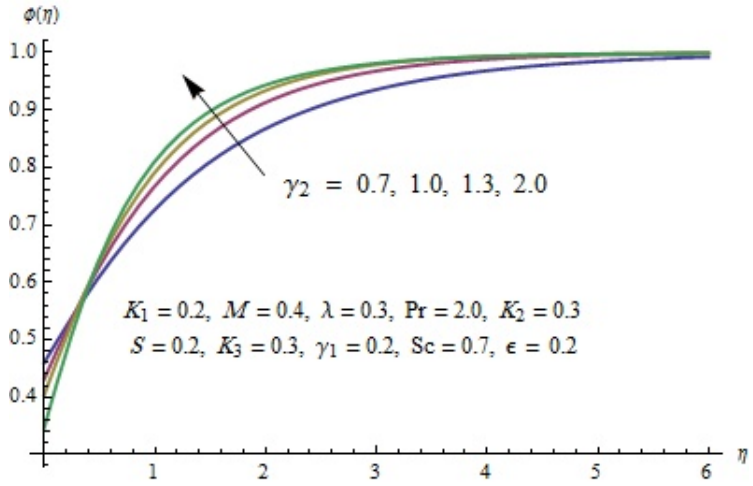

Fig. 12: Effect of γ_2 on $\phi(\eta)$

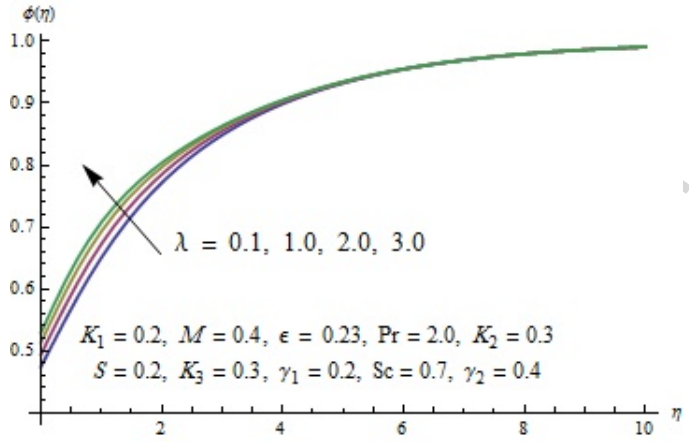

Fig. 13: Effect of λ on $\phi(\eta)$

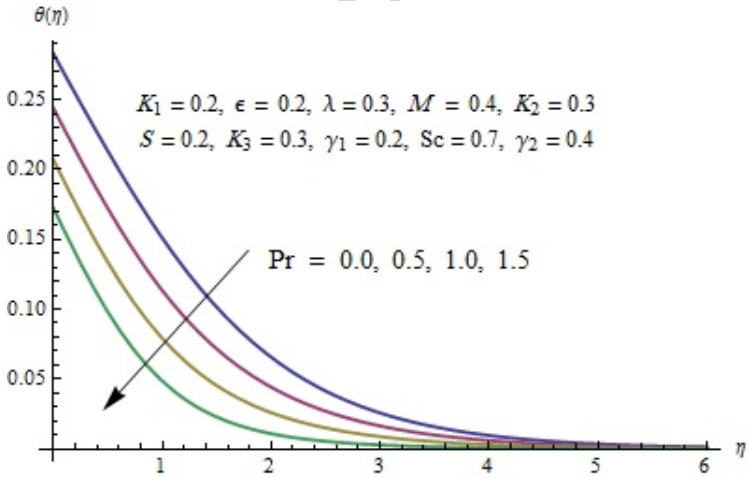

Fig. 14: Effect of Pr on $\theta(\eta)$

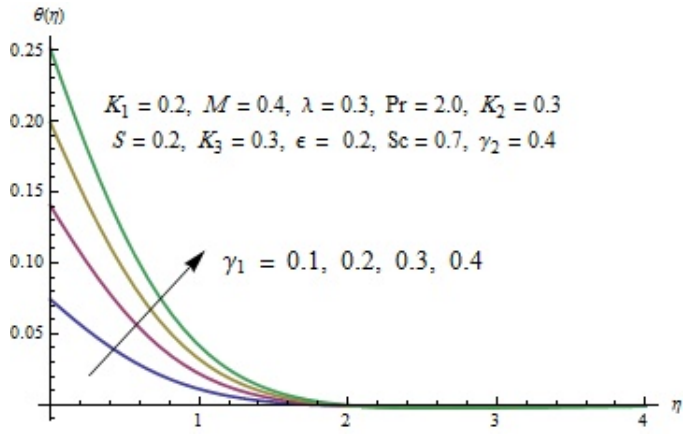

Fig. 15: Effect of γ_1 on $\theta(\eta)$

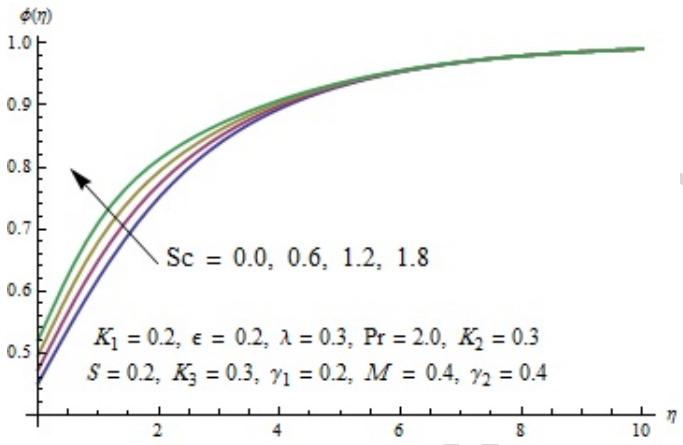

Fig. 16: Effect of Sc on $\phi(\eta)$

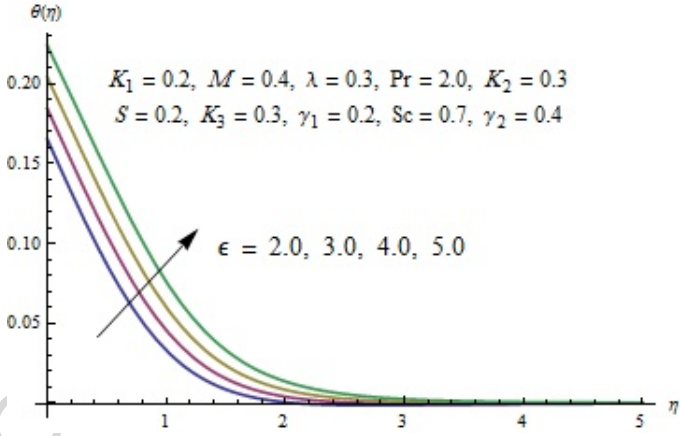

Fig. 17: Influence of ϵ on $\theta(\eta)$

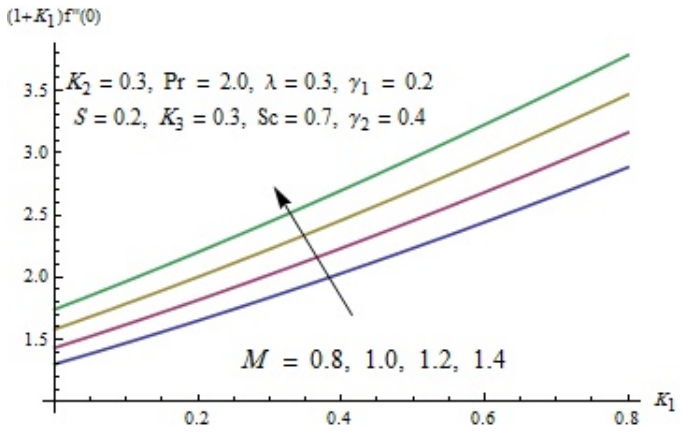

Fig. 18: Effects of M and K_1 on Skin friction

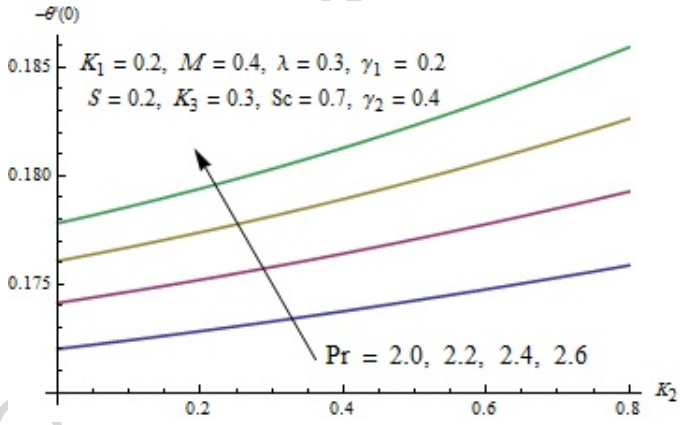

Fig. 19: Effects of Pr and K_2 on Nusselt number

Highlights

- Flow of 3D Maxwell fluid with Homogeneous and heterogeneous reactions is studied.
- Effects of 3D Cattaneo-Christov heat flux are also considered.
- Analytical solution is obtained using Homotopy Analysis method.
- Temperature field is growing function Biot number.
- Heat generation/absorption parameter causes an increase in temperature field.